

## Research Article

Theme: Pediatric Drug Development and Dosage Form Design  
Guest Editors: Maren Preis and Jörg Breitzkreutz

# Colorimetry as Quality Control Tool for Individual Inkjet-Printed Pediatric Formulations

Henrika Wickström,<sup>1,4</sup> Johan O. Nyman,<sup>1</sup> Mathias Indola,<sup>1</sup> Heidi Sundelin,<sup>2</sup> Leif Kronberg,<sup>2</sup> Maren Preis,<sup>1</sup> Jukka Rantanen,<sup>3</sup> and Niklas Sandler<sup>1</sup>

Received 31 May 2016; accepted 15 August 2016; published online 13 October 2016

**Abstract.** Printing technologies were recently introduced to the pharmaceutical field for manufacturing of drug delivery systems. Printing allows on demand manufacturing of flexible pharmaceutical doses in a personalized manner, which is critical for a successful and safe treatment of patient populations with specific needs, such as children and the elderly, and patients facing multimorbidity. Printing of pharmaceuticals as technique generates new demands on the quality control procedures. For example, rapid quality control is needed as the printing can be done on demand and at the point of care. This study evaluated the potential use of a handheld colorimetry device for quality control of printed doses of vitamin Bs on edible rice and sugar substrates. The structural features of the substrates with and without ink were also compared. A multicomponent ink formulation with vitamin B<sub>1</sub>, B<sub>2</sub>, B<sub>3</sub>, and B<sub>6</sub> was developed. Doses (4 cm<sup>2</sup>) were prepared by applying 1–10 layers of yellow ink onto the white substrates using thermal inkjet technology. The colorimetric method was seen to be viable in detecting doses up to the 5th and 6th printed layers until color saturation of the yellow color parameter (b\*) was observed on the substrates. Liquid chromatography mass spectrometry was used as a reference method for the colorimetry measurements plotted against the number of printed layers. It was concluded that colorimetry could be used as a quality control tool for detection of different doses. However, optimization of the color addition needs to be done to avoid color saturation within the planned dose interval.

**KEY WORDS:** fixed-dose combinations; handheld colorimeter; inkjet printing; pediatric medicine; quality control.

## INTRODUCTION

Pediatric patients are often prescribed off-label, unlicensed, or compounded products due to the lack of appropriate products on the market (1). The quality of the compounded products is usually poorer, due to the lack of standards with regard to quality assurance of these formulations (2). Stability issues, changed release properties, and the palatability are rarely considered and might also sometimes be totally ignored (2, 3). Innovative research efforts have therefore been made to achieve

solid dosage forms that are age-appropriate. The main aim has been to develop easily administrable formulations with dosing flexibility and acceptable taste. The call has been answered by introducing orodispersible films (ODFs), that disintegrate in the oral cavity and mini-tablets ( $\leq 3$  mm) (4, 5). For instance, mini-tablets of 2 mm were concluded, in a clinical study for patients from 6 months to 6 years, to be a valuable alternative to syrup (6). Both the ODFs and mini-tablets have shown to enable loading of low-dose active pharmaceutical ingredients (APIs). It is known that incorporation of drug influences the mechanical properties of the ODFs. Due to this, a comparative study was performed investigating the physical properties of the API loaded films achieved with two different manufacturing techniques [7]. The drug was either incorporated into the film solution before solvent casting or by applying a drug containing ink, by inkjet technology, onto a drug-free film. Inkjet printing was found to be the favorable option, suggesting that the API is present only on top or in the top layer of the ODF resulting in more durable mechanical properties of the film compared to the solvent casted film, in which the API is incorporated.

<sup>1</sup> Pharmaceutical Sciences Laboratory, Faculty of Science and Engineering, Åbo Akademi University, Artillerigatan 6A, FI-20520, Åbo, Finland.

<sup>2</sup> Laboratory of Organic Chemistry, Faculty of Science and Engineering, Åbo Akademi University, Turku, Finland.

<sup>3</sup> Department of Pharmacy, Faculty of Health and Medical Sciences, University of Copenhagen, Copenhagen, Denmark.

<sup>4</sup> To whom correspondence should be addressed. (e-mail: henrika.wickstrom@abo.fi)

In the future, solid dosage forms could be printed at the point of care (PoC) allowing late-stage customization, where the specific needs of the treated child is taken into consideration (8, 9). Age- and weight-appropriate doses could easily be achieved, and thus, problems related to compounding of licensed drugs prescribed to children could be avoided. Printing technologies have shown to enable rapid production of flexible doses with high dose accuracy (10–12) and tailored release properties (13). Dose accuracy is easily achieved as small droplets (10–75 pl) are ejected from the inkjet printers and different release properties are obtained by application of one or more passes of a polymeric solution on top of the printed APIs by means of flexography printing. Addition of for example sweeteners or solubility enhancers into the polymeric solution is known to improve the palatability of solvent-casted ODFs (4). Vitamins (Table I) (14), food supplements, low-dose drugs with the need for dose adjustment, and drugs with a small therapeutic window are especially applicable choices to use, when formulating printed drug delivery systems for children. APIs and edible and non-edible substrates used in printing studies so far are well summarized by Kolakovic *et al.*, (15) and Alomari *et al.*, (16).

Characterization of the solid state of the drug in the printed formulations has so far been shown to be challenging. Efforts in the determination of the solid state by X-ray diffraction, infrared (IR), near-infrared (NIR), and Raman spectroscopy has been reported unsuccessful, most likely due to the low doses and/or the interference caused by the carrier matrix (11). Yet, first approaches to implement quality control of the printed dose have successfully been done. NIR-hyperspectral imaging showed to be a reliable, rapid, and non-destructive method to control dose titrations (17), and reflectance IR spectroscopy was applicable as a process analytical method allowing in-line monitoring and real-time adjustment of the drug content during solvent casting of API-containing films (18).

Colorimetry has been used for quality assurance applications in food industry, for shade matching in dentistry and for soil characterization in the field of geology, to name a few examples (19–22). In food industry, color is the most important quality attribute for the customer, which naturally has led to the need and utilization of an objective way to define the color during the supply chain (23). For instance, the color change caused by variations in the storage temperature has been examined for bananas (24). The qualitative appearance factor (color) was correlated to the quantitative amount of carotenoids present in the banana pulp at different storage conditions. Colorimetric methods are also utilized in the pharmaceutical field. For instance, the performance of two photometric handheld devices was evaluated in detecting counterfeit antimalarial tablets, having a colorimetric method as reference (25). Both devices

were able to detect the falsified or degraded tablets. Color is in general used in the pharmaceutical industry to ease identification of, e.g., batches (26), but also to indicate different dose strengths of the same product or fixed-dose combinations. The color, size, and medication type might also have an impact on the perceived effectiveness of a drug (27). Furthermore, easily administered medicine of the preferred color could have a positive impact on the patient compliance and the medical treatment of the pediatric population.

Colors are based on perception and interpretation done by individuals. The human is able to distinguish between three main colors and is therefore defined as a trichromatic organism (23). Photoreceptor cells, cones, in the retina are sensitive to light of short (420–440 nm), middle (530–540 nm), and long (560–580 nm) wavelengths (reflected or emitted from an object), resulting in a sensation of blue, green, and red, respectively. These three color components are also defined as tristimulus values. Different color spaces are mathematically composed of the tristimulus values. These are (1) hardware-oriented, (2) human-oriented, and (3) instrumental color spaces. Red, green, blue (RGB) and cyan, magenta, yellow, black (CMYK) are two of the most popular hardware-oriented spaces. RGB is mainly used in cameras and CMYK is used in television transmission and printing. The human-oriented space elucidates differences related to tints, shades, and tones. Hue is an attribute of visual perception of an area corresponding to red, green, blue, yellow, or a combination between two colors. Instrumental color spaces were standardized in 1931 by the Commission Internationale d'Eclairage (CIE) and was further improved in 1976 with the introduction of the CIELAB color space (20, 28). This color space is most frequently used in food industry, due to the similarities to the human perception of color (28). The  $L^*$ ,  $a^*$ , and  $b^*$  abbreviations stand for lightness, green/red, and blue/yellow color opponents, respectively (Fig. 1) (29, 30). The lightness value ranges from 0 to 100 (dark to light), while the color opponents range from –120 to 120 (28).  $\Delta E^*_{ab}$  is a numerical value describing the difference in color illumination between a measured sample ( $L^*_1, a^*_1, b^*_1$ ) and a reference ( $L^*_0, a^*_0, b^*_0$ ) (Eq. 1) (30). Light intensity is an important factor affecting the measurement outcome. It depends on both the intensity and spectral distribution of the illuminated light and the spectral distribution of the object reflectivity. D65 is a standard illuminant corresponding to daylight and thus widely used (30,31). The measurement geometry is also important to consider when measuring color illumination. This has been standardized, and  $45^\circ:0^\circ$  has been evaluated to resemble the human perception of colors, meaning that the light source reaches the sample perpendicularly and reflects the light with a  $45^\circ$  angle. In general, to be able to obtain accurate results using a colorimeter, the measured area should preferably be flat, clean, and dry (30). Completely opaque samples are preferred, and the measurement area should be large enough to cover the sample orifice of the instrument used.

Printing of pharmaceuticals has emerged as a potential manufacturing method to produce flexible, age- and weight-appropriate doses for pediatrics. Yet, there are no generally accepted guidelines for quality control of these printed

**Table I.** Recommended B<sub>1</sub>, B<sub>2</sub>, and B<sub>6</sub> Intake for Children (14)

Age	Vitamins (mg/day)		
	Thiamin (B <sub>1</sub> )	Riboflavin (B <sub>2</sub> )	Pyridoxine (B <sub>6</sub> )
0–6 (months)	0.2	0.3	0.1
7–12 (months)	0.3	0.4	0.3
1–3 (years)	0.5	0.5	0.5
4–8 (years)	0.6	0.6	0.6
9–13 (years)	0.9	0.9	1.0

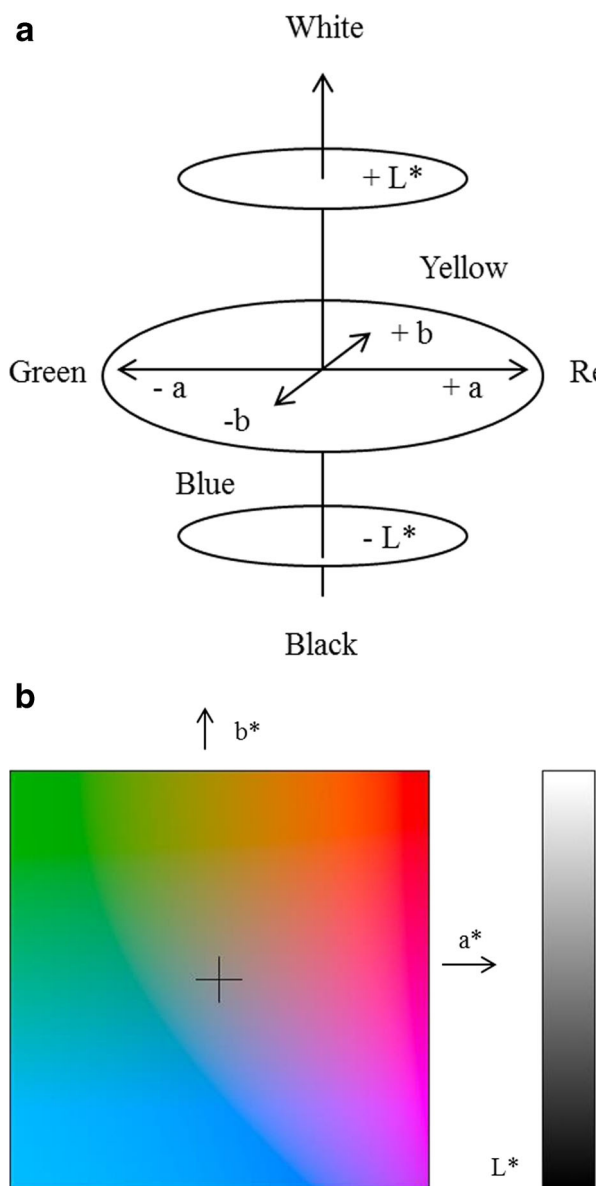


**Fig. 1.** a. CIELAB color space, modified (29). b.  $L^*a^*b^*$  chart, image captured from software (30)

pharmaceutical formulations. The aim was to study the correlation of the color intensity of the printed doses with the printed number of layers. Liquid chromatography mass spectrometry (LC-MS) was used as the reference method for dose quantification. Determination of the surface roughness of the substrates with and without ink was carried out using scanning white light interferometry (SWLI) to support the colorimetry results. The overall objective was to evaluate if the handheld colorimeter could be used as a cost-effective and fast quality assurance tool for dose control of printed fixed-dose combinations, in particular for pediatric low-dose preparations, and to study the substrate roughness as a means of ink deposition.

## MATERIALS AND METHODS

Thiamine hydrochloride, vitamin B<sub>1</sub> (Fluka, Germany), riboflavin 5'-monophosphate sodium salt, vitamin B<sub>2</sub> (Sigma-Aldrich, France), nicotinamide, vitamin B<sub>3</sub> (Sigma-Aldrich,

China), and pyridoxine hydrochloride and vitamin B<sub>6</sub> (Sigma-Aldrich, Germany) were used as APIs in this study. A commercially available edible ink (Canon CLI-521 Series, DECO Enterprises LDR, UK) applicable for printing with Canon printers, was used as solvent. The ink was yellow and consisted of water, glycerol, tartrazine (1.5%), propylene glycol, and citric acid. Copy paper (CP) (Staples A4 copy paper, Staples Europe B.V., the Netherlands) and rice paper (RP) (Easybake® edible rice paper, N.J. Products Ltd., UK) were used as substrates for printing. RP consisted of potato starch, vegetable oil, and water. Sugar paper (SP) consisted of starches (E1422, E1412), maltodextrin, glycerine, sugar, water, stabilizers (E141, E471), food color (E171), citric acid, flavors, preservative (E202), and sucralose.

## Ink Formulation

An ink cocktail with B<sub>1</sub>, B<sub>2</sub>, B<sub>3</sub>, and B<sub>6</sub> was prepared by dissolving the vitamins in the yellow edible ink (Deco Enterprises Ltd., Sutton Valence, Kent, UK). The cartridge containing the edible yellow ink was emptied, washed, and refilled with vitamin containing ink using a syringe and needle. The concentrations of B<sub>1</sub>, B<sub>2</sub>, B<sub>3</sub>, and B<sub>6</sub> in the cocktail were 10, 10, 20, and 10 mg/mL, respectively.

## Printing

An unmodified thermal desktop inkjet printer Canon Pixma iP3600 (Canon Inc., Japan), with the paper loaded face-up, was used for printing. To allow ink ejection only from the yellow cartridge, manual color adjustment was applied in the software. The CMYK values were set at 0, 0, 1, and 0. No ink development was needed, since the ink was designed to be used with Canon printers. During the printing process, ink was applied onto an area of 4 cm<sup>2</sup> and dose escalation was achieved by printing 1–10 layers. The printed layers were allowed to dry for 15 min in between the printing passes. One vitamin ink was used for all printing tasks. Printing was initiated by printing doses on CP (reference substrate) and continued by printing doses on edible RP and SP. The printed doses with vitamin Bs were stored at room temperature and protected from light prior to the content analysis.

## Colorimetry Measurements of Printed Doses

A digital handheld colorimeter (CLM-194, Eoptis, Trento, Italy) was used to study the color illumination of the printed doses ( $n=3$ ). The results of the color measurements were presented as  $L^*a^*b^*$  values ( $\pm$  SD) of the CIELAB system having D65 set as illuminant and CIE1931-2° as observer. The measurement geometry of the device was circumferential with 45° illumination and 0° viewing, according to CIE14:2004 and ASTM E1164. Integrated light-emitting diodes (LEDs) were the illumination source of the colorimeter. A white reference standard was used to calibrate the colorimeter. The color illumination difference measured between the printed dose ( $L_1, a_1, b_1$ ) and reference ( $L_0, a_0, b_0$ ) was presented as CIELAB  $\Delta E^*_{ab}$  values. The first printed layer was captured as a measurement reference, whereafter the series of vitamin doses (2–10 layers) were measured. The parameter  $L^*$  corresponds to lightness ( $L^*=0$  is black and

$L^* = 100$  is light). Color opponents  $a^*$  and  $b^*$  correspond to green ( $-a^*$ ), red ( $+a^*$ ), blue ( $-b^*$ ), and yellow ( $+b^*$ ). The colorimeter values were plotted against printed layers and measured doses. The linearity of the color intensity ( $\Delta E^*_{ab}$ ) escalation for the formulations was reported. The conditions needed for making an accurate measurement such as the samples being dry, flat, or opaque was ensured when conducting the colorimetric measurements.

### Reference Method and Sample Preparation for Determining the Drug Content (LC-MS)

LC-MS was used as a reference method for the presented colorimetric analysis method. The instrument setup consisted of a 1100 series Agilent high-performance liquid chromatograph, equipped with a binary pump, a vacuum degasser, an autosampler, and a thermostated column oven (Agilent, Santa Clara, CA, USA). Nitrogen 5.0 gas was used both as nebulizing gas (40 psi) and drying gas (10 L/min, 350°C). Mass spectrometric detection of the vitamins was performed using an Agilent MSD Trap SL ion trap mass spectrometer equipped with an electrospray ionization source (Agilent Technologies, Palo Alto, CA, USA). Raw data collection was done using the ChemStation for LC 3D Systems software, rev. B.01.03 (Agilent, Santa Clara, CA, USA). Further data analysis was performed with Microsoft Excel 2010 software (Microsoft Corporation, USA).

A previously presented method was used for the extraction of vitamin Bs in this study (32). Prior to the analysis, the printed samples were cut out leaving a 5 mm boarder of the substrate around the printed area, immersed in 10 mL of 0.1% aqueous formic acid, and sonicated for 15 min at room temperature. The doses of vitamin Bs printed on SP were centrifuged and filtrated through a 0.2  $\mu\text{m}$  polytetrafluorethylene membrane. LC-MS analysis was initiated immediately after the sample preparation.

Separation of the vitamins was performed on an Atlantis T3 analytical column (3  $\mu\text{m}$ , 2.1  $\times$  100 mm; Waters, Ireland) equipped with a pre-column of the same material (3  $\mu\text{m}$ , 2.1  $\times$  100 mm). The column oven was thermostated at 30°C during the analysis. Mobile phases utilized in the analysis consisted of 0.1% aqueous formic acid (A) and 0.1% formic acid in 50:50 ACN:MeOH (B). Optimal separation of the analytes was obtained using gradient elution, starting with 1% of B and ending with 95% of B. The flow rate was set to 0.3 mL/min, the injection volume was 30  $\mu\text{L}$ , and the run time was 25 min. Mass spectrometric detection of the separated vitamin Bs was performed in positive mode. Analytical ions ( $m/z$ ) were 265, 457, 123, 170, and 152 for B<sub>1</sub>, B<sub>2</sub>, B<sub>3</sub>, B<sub>6</sub>, and paracetamol (internal standard), respectively. Drug content of the printed vitamin B (B<sub>1</sub>, B<sub>2</sub>, B<sub>3</sub>, and B<sub>6</sub>) samples was determined for all printed doses in triplicate. Quantification of vitamin Bs, based on the peak areas of the analytical ions, was performed using five-point calibration curves in the range 1–20  $\mu\text{g/mL}$  for each vitamin with 5  $\mu\text{g/mL}$  paracetamol as internal standard. The repeatability was determined by injecting 10  $\mu\text{g/mL}$  ( $n = 10$ ) of the vitamins and by calculating the relative standard deviations. The matrix effect was evaluated by comparing five analyses of a solution containing the four vitamins dissolved in distilled water with five analyses of a solution containing the substrate printed with five layers of the edible ink containing the four vitamins.

### Surface Texture and Substrate Thickness Analysis

Surface texture analysis was performed on all samples using a custom-made SWLI instrument. The instrument consisted of a Nikon reflective microscope frame, equipped with a 10 $\times$  Mirau interferometry objective (Nikon IC EPI Plan DI, Japan), a 100- $\mu\text{m}$  piezoelectric z-scanner (Physik Instrumente P-721 PIFOC<sup>®</sup>, Karlsruhe, Germany), a high-resolution CCD camera (Hamamatsu ORCA-Flash 2.8 CMOS, Hamamatsu City, Japan), and two motorized translation stages (Standa 8MTF-102LS05; Vilnius, Lithuania). As white light source, a standard halogen lamp was used. The total magnification of this setup was  $\times 6.3$ . Scanning and data acquisition was controlled with an in-house built C++-based software. 3D image construction and 3D data analysis were performed using the commercial MountainsMap<sup>®</sup> Imaging Topography 7.2 software (Digital Surf, Avencon, France). Surface texture of the samples, based on the root mean square height of the surface ( $S_q$ ), was calculated according to the ISO 25178 standard using the MountainsMap<sup>®</sup> Imaging Topography 7.2 software. The obtained topographical information of the sample surfaces was furthermore separated into waviness components ( $S_q\text{-W}$ , describing large-scale surface texture changes) and roughness components ( $S_q\text{-R}$ , gives indications on the nature of the material) using the same software. Plain substrate surface and surfaces of 5 and 10 printed layers were studied. Substrate thickness measurements were performed in triplicate using a micrometer device (Lorentzen & Wettre, Stockholm, Sweden). Substrate samples of 14  $\times$  14  $\text{cm}^2$  were cut and measured at five spots.

## RESULTS

### Colorimetric Monitoring of Inkjet-Printed Fixed-Dose Combinations

Fixed-dose content was measured using a colorimetric method by monitoring color intensity of the doses achieved by deposition of different numbers of layers (Fig. 2). The color intensity of the ink solution was gained from the initially colored edible ink containing 1.5% of tartrazine and the added vitamin B<sub>2</sub>. The lightness parameter ( $L^*$ ) and the yellow color component ( $+b^*$ ) were the main parameters that gave rise to color intensity differences ( $\Delta E^*_{ab}$ ) of the doses as a function of printed layers (Fig. 3).  $L^*$  values slightly decreased, while the color parameters changed slightly towards green ( $-a^*$ ) and more towards yellow ( $+b^*$ ). The flattening of the color intensity difference values was due to the saturation of the yellow color component  $+b^*$  in the printed doses (Fig. 3b).

The largest numerical difference of the  $\Delta E^*_{ab}$  values was observed between the 1st printed layer (reference) and the two-layer dose. The substrates as such were not used as reference areas as the difference between the color component values ( $a^*$  and  $b^*$ ) of the substrate and the 1st printed layer was too high (Fig. 3a, b), thus giving rise to non-detectable color differences with the analysis instrument used.

Color intensity difference values ( $\Delta E^*_{ab}$ ) increased up to the 5th printed layer for doses on SP and 6th printed layer for doses on CP and RP (Fig. 3c). This flattening of the  $\Delta E^*_{ab}$  value, as mentioned earlier, was due to the saturation of the yellow color component. The  $\Delta E^*_{ab}$  value was observed to be higher for RP ( $\Delta E^*_{ab} = 52$ ) and lower for SP and CP



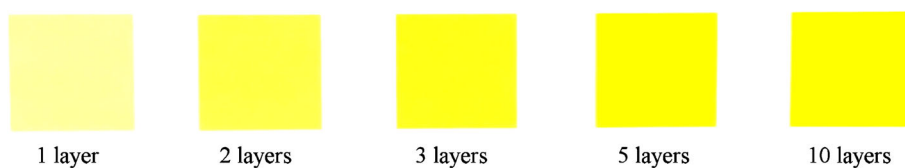


**Fig. 2.** Increasing doses of vitamin Bs inkjet-printed on CP. From left to right, 1, 2, 3, 5 and 10 printed layers

( $\Delta E^*_{ab} = 38$  and  $39$ , respectively). To statistically evaluate the linearity, the coefficient of regression ( $R^2$ ) was calculated based on the  $\Delta E^*_{ab}$  values as a function of printed layers, before the saturation of the yellow color component ( $b^*$ ) was reached. The linearity of the colorimetric method for the different printed formulations was  $R^2 = 0.9496$  (CP),  $R^2 = 0.9609$  (RP), and  $R^2 = 0.9918$  (SP).  $\Delta E^*_{ab}$  values plotted against the quantified dose of  $B_2$  reveal that the printed dose deviated from substrate to substrate. The obtained dose was the lowest for CP and highest for SP (Fig. 3d).

Dose escalation was obtained as a function of printed layers ( $n = 10$ ). However, the amount of vitamin B addition per layer decreased as the number of layers increased on all substrates (Fig. 4). The best linearity was observed for vitamin  $B_2$  and  $B_6$  printed on CP. However, the greatest dose variability between the different substrates was seen for  $B_2$ .

Linear calibration curves exceeding  $R^2 = 0.97$  were obtained for the LC-MS reference method ( $B_1$ ,  $R^2 = 0.9865$ ;  $B_2$ ,  $R^2 = 0.9841$ ;  $B_3$ ,  $R^2 = 0.9735$ , and  $B_6$ ,  $R^2 = 0.9916$ ) by plotting the ratio

of the peak areas of the analyte and the internal standard against the concentration of the analyte. The deviation of the repeatability of the LC-MS method was determined to be 5, 6, 10, and 8% for  $B_1$ ,  $B_2$ ,  $B_3$ , and  $B_6$ , respectively. No matrix effect was found for the CP and RP setups. However, correction factors of 1.90, 1.19, 2.18, and 1.49 were used for all vitamins printed on SP. The detection limit for the LC-MS instrument was 5 ng/mL for  $B_1$  (157 pg on column), 7 ng/mL for  $B_2$  (196 pg on column), 0.6 ng/mL for  $B_3$  (17 pg on column), and 0.1 ng/mL for  $B_6$  (4 pg on column).

### Surface Properties of Printed Samples and Substrates

Differences with regard to substrate roughness (Sq-R), waviness (Sq-W), thickness, and specific volume were observed for all three substrates (Table II). The surface texture of the substrate matrixes were imaged using SWLI and analyzed with regard to the root mean square height of the surface (Sq), which defines the surface texture of the sample. The roughness

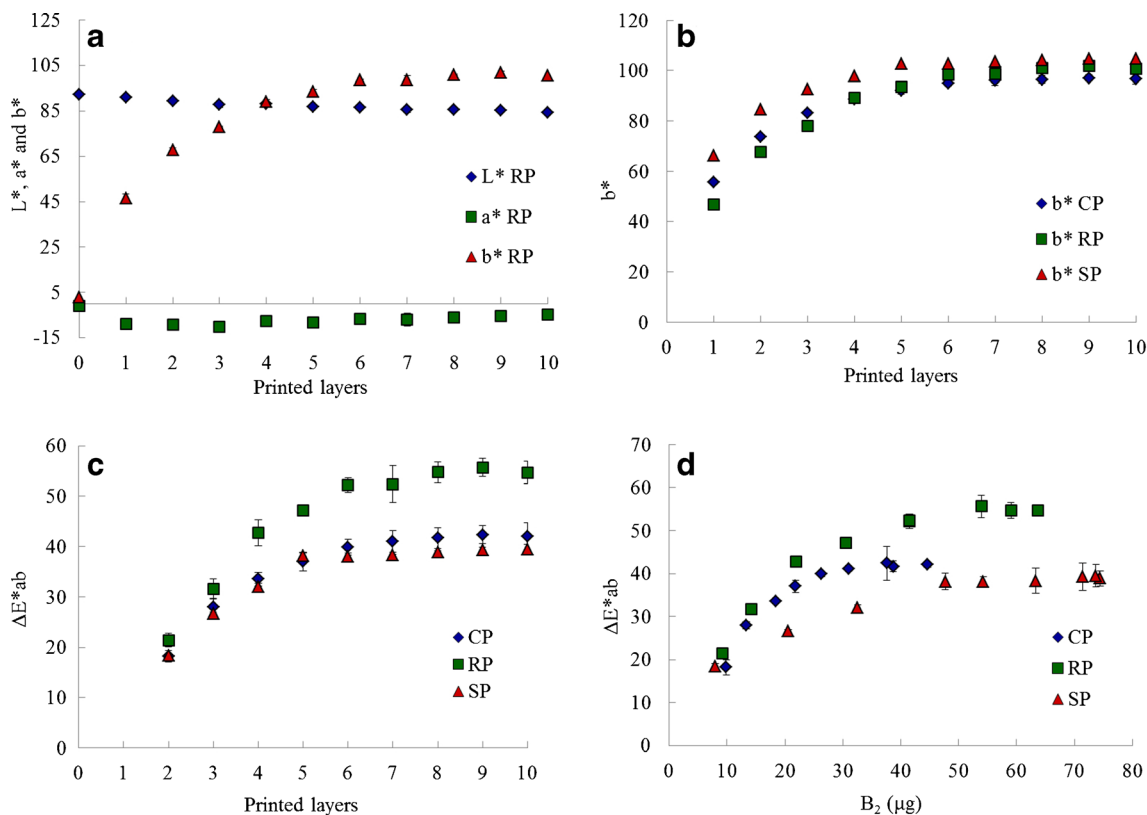


**Fig. 3.** **a.**  $L^*$ ,  $a^*$ , and  $b^*$  values for the printed RP samples plotted against the number of printed layers. Values for RP without ink (0 layers) are also included in the graph. **b.**  $b^*$  values displayed as a function of printed layers on CP, RP, and SP. **c.**  $\Delta E^*_{ab}$  values of the doses (2–10 layers) on CP, RP, and SP having the first printed layer as reference. **d.**  $\Delta E^*_{ab}$  values for 2–10 printed layers of riboflavin ( $B_2$ ) plotted as a function of dose ( $\mu\text{g}$ ) on CP, RP, and SP

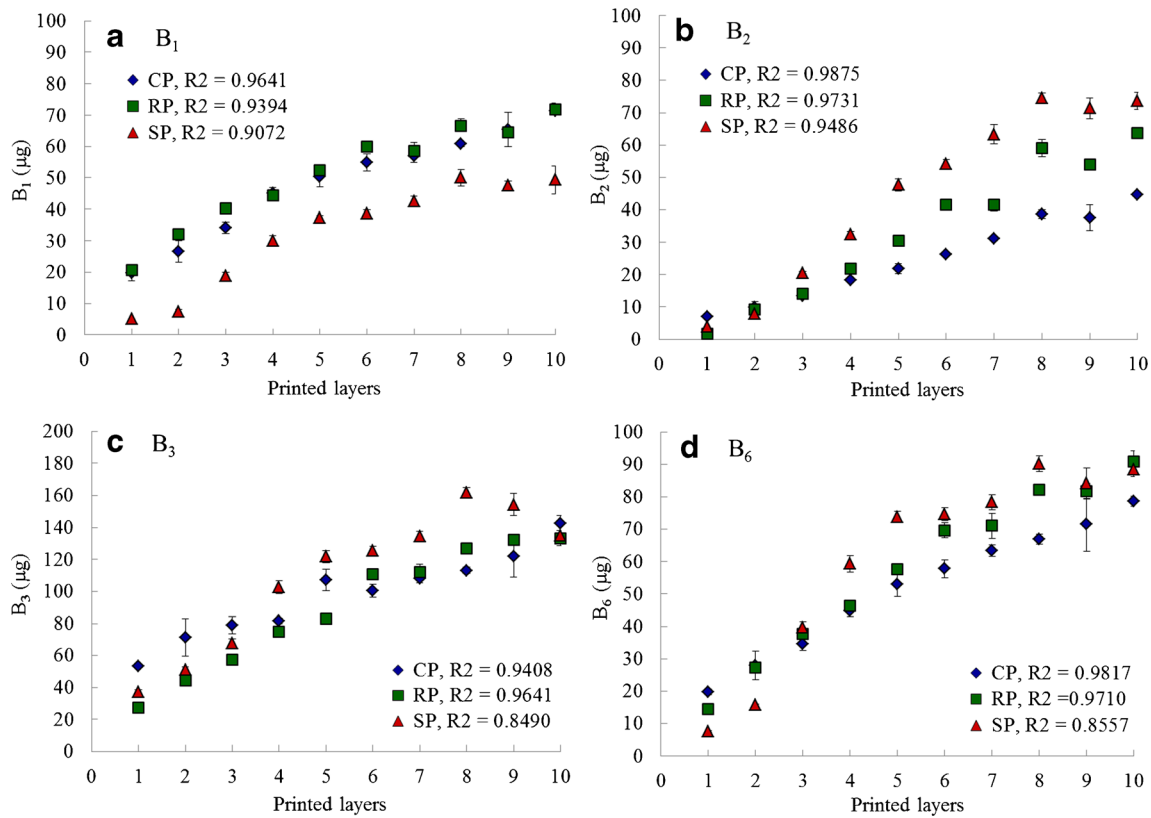


**Fig. 4.** The quantified doses of B<sub>1</sub>(a), B<sub>2</sub> (b), B<sub>3</sub>(c), and B<sub>6</sub> (d) as a function of printed layers on CP, RP, and SP

component (Sq-R), indicating the nature of the material, was the most dominating component for all substrates. The waviness component (Sq-W), describing large-scale surface texture changes, was highest for RP without ink. CP was the thinnest ( $\sim 100 \mu\text{m}$ ) and smoothest substrate, followed by RP ( $\sim 290 \mu\text{m}$ ) and SP ( $\sim 320 \mu\text{m}$ ) according to the measured thickness and Sq values. The highest specific densities were calculated for the CP and RP substrates. By visual perception, the RP seemed to be the roughest and the most porous substrate. Yet, the perception of the roughness was proven wrong according to the measured Sq values. RP was, however, the substrate with the highest specific volume. SP was the most compact and dense substrate.

The SWLI image captures exposed the fibrous nature of both the pure and printed CP and RP (Fig. 5). Regardless of the fiber structures, the highest roughness value was observed for the pure SP consisting of various sugar-based ingredients. Application of ink gave rise to an increase in the Sq-R values for CP and RP, due to the observed swelling behavior of the fibers in the matrix. For example, application of 10 layers of ink on CP increased the surface roughness with more than  $5 \mu\text{m}$ . An even greater increase in roughness of almost  $10 \mu\text{m}$  was measured for RP. The Sq-R value of SP was seen to decrease as the aqueous ink was applied onto the matrix. This was most likely due to dissolution of the top layer of the sugar substrate.

**Table II.** Results of the Surface Texture Analysis, Thickness Measurements and Specific Volume Calculations of Substrates with and without Ink

Substrate	Sq ( $\mu\text{m}$ ) <sup>a</sup>	Sq-W ( $\mu\text{m}$ ) <sup>a</sup>	Sq-R ( $\mu\text{m}$ ) <sup>a</sup>	Thickness ( $\mu\text{m}$ ) <sup>b</sup>	Specific volume ( $\text{cm}^3/\text{g}$ ) <sup>b</sup>
CP					
0 layers	7.87	1.52	7.57	$99.4 \pm 2.29$	1.33
5 layers	10.20	1.46	9.92	–	–
10 layers	13.50	1.94	13.00	–	–
RP					
0 layers	11.50	3.80	10.30	$288.9 \pm 2.46$	3.76
5 layers	19.90	6.59	18.30	–	–
10 layers	21.90	7.17	20.10	–	–
SP					
0 layers	16.00	1.73	15.90	$318.3 \pm 1.85$	0.73
5 layers	14.60	1.53	14.40	–	–
10 layers	14.60	1.40	14.50	–	–

<sup>a</sup>  $n = 1$

<sup>b</sup>  $n = 3$

$$\Delta E^*_{ab} = \sqrt{(L^*_1 - L^*_0)^2 + (a^*_1 - a^*_0)^2 + (b^*_1 - b^*_0)^2} \quad (1)$$

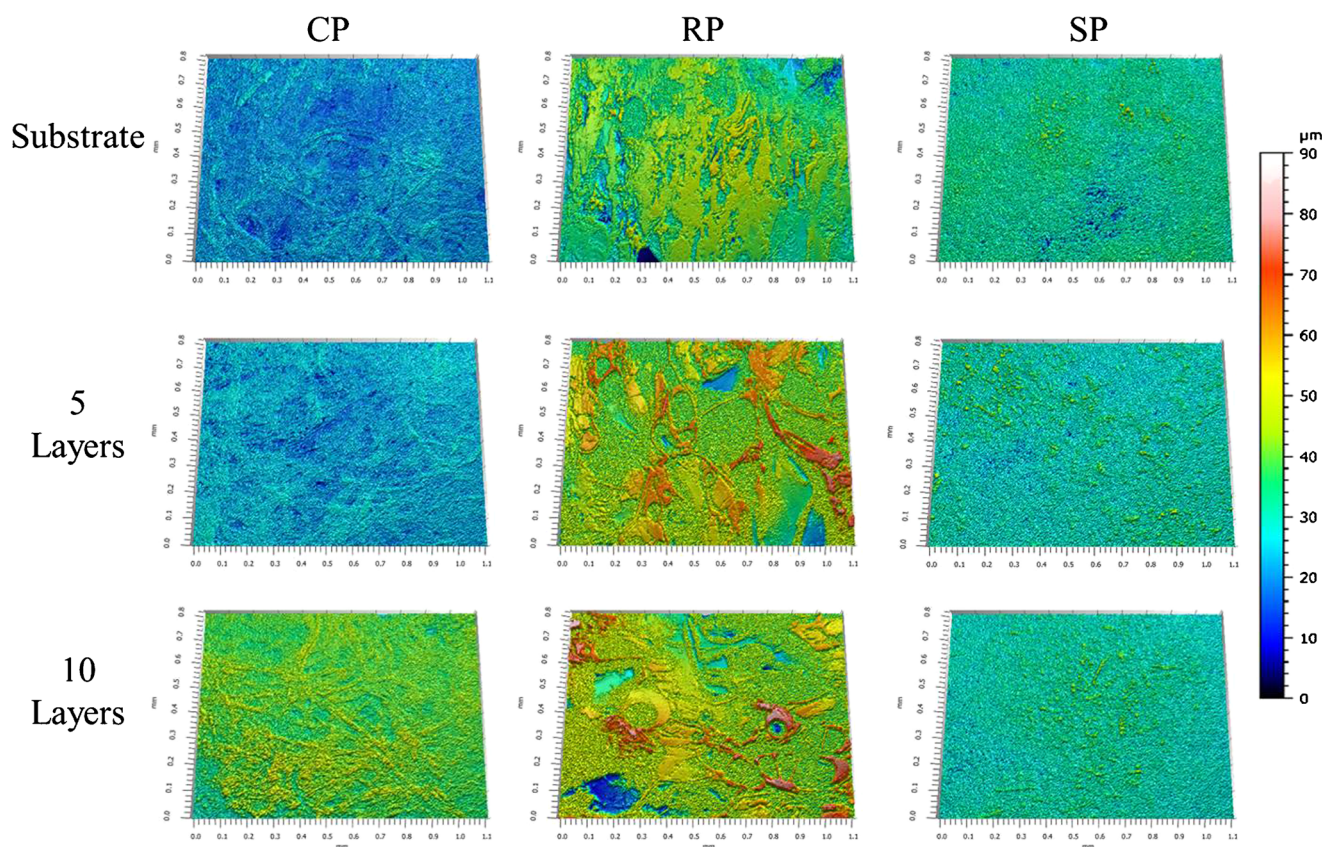


**Fig. 5.** 3D images of only substrate (CP, RP, and SP) and substrate with 5 and 10 printed layers of ink. All images are of  $1.1 \times 0.8$ -mm size. The color of the specimens correspond to the color of the gradient bar, which is equal to the measured height difference (0-90- $\mu\text{m}$ )

## DISCUSSION

### Dose and Stability

Inkjet printing is known to be applicable to accurately dispense droplets in the picoliter range onto different substrate matrixes (32, 33). This technology would enable manufacturing of low-dose drugs according to the needs of the pediatric population, a population which usually is often given off-label medicines or compounded medicines due to the lack of age- or weight-appropriate doses (2). The printed doses on RP were 35.9, 21.2, and 90.8% of the recommended  $B_1$ ,  $B_2$ , and  $B_6$  intake, respectively, for newborn to 6-month-old children (Table I) (14). In order to print higher doses in the future, the initial vitamin concentration of the ink can be increased. Solubility of the API in the printable solvent mixture and/or the lack of an ink-absorbing substrate are known to limit the possibilities of dose escalation to a certain extent. However, the solubility of the vitamin Bs in the aqueous solvent mixture would most probably not be an issue.

Dose escalation was achieved by printing layers of ink on top of each other ( $n = 10$ ). The LC-MS results revealed that the addition of vitamins per layer decreased as the number of layers increased on all substrates (Fig. 4). Similar dose wear-offs have been reported earlier for inkjet-printed doses with both face-down and face-up substrate feeding mechanisms of the printers used (10, 34). The dose escalation with best linearity was determined for  $B_1$ ,  $B_2$ , and  $B_6$  on the reference substrate, CP. A previously conducted dose escalation study

showed similar  $R^2$  values for the CP, while the linearity was poorer for the doses on edible ODFs and impermeable transparency films (10). The superior dose escalation results shown for CP were expected, since the substrates are designed, as a means of absorption properties and thickness, for printing purposes with office printers. RP turned out to be the most promising edible substrate with regard to dose escalation.

The printed doses of vitamin  $B_2$  on CP and RP were lower compared to the vitamin  $B_1$  and  $B_6$  doses. Vitamin  $B_2$  is known to undergo degradation through different mechanisms (35). Exposure to light, temperature, and water has been reported to cause degradation. The printed samples were protected from light after the printing task and during drying. Degradation of vitamin  $B_2$  was possibly initiated already after dissolving the vitamin into the aqueous, edible ink. The drying time of the doses on the substrates with different properties might also have played a role, especially for the higher doses when several printed layers were applied. Thermal degradation could not be excluded either, since the ejection of a droplet in thermal printers is based on rapid heating of a resistive element up to 350–400°C (36). This causes a vapor bubble to form, which in turn results in droplet ejection from the nozzle of the print head. Significant degradation percentages (>20%) have been reported for aqueous solutions of  $B_2$ , when being heated for 40 min at 150°C (35). However, degradation of  $B_2$  initiated by high temperature during the printing process was not of major concern, thanks to the fast heating step ( $\mu\text{s}$ ) of the printing process (37). Based on the results from this study, it is



recommended to get proper understanding on how processing (i.e., temperature) and different storage conditions affect the formulation containing only one vitamin or drug, before moving to multicomponent formulations. Special care should also be taken when planning and performing colorimetric measurements in the future with vitamin B<sub>2</sub>. A decrease in color intensity ( $\Delta E^*_{ab}$ ) was for instance reported after exposing vitamin B<sub>2</sub> to light (38). The decrease was observed to occur with a 24 h delay.

### Colorimetry and Colorant Addition

Color is generally used in pharmaceuticals to ease the identification of different medicines or different doses (26). The color can be obtained by addition of a colorant or by having a colored API in the formulation. Apart from distinguishing between dose strength, colors have also been studied to indicate solvent presence or degradation of the API (26, 39). Vitamin B<sub>2</sub> is a natural colorant used in pharmaceuticals (40). The vitamin by itself would have enabled visualization of the printed area on the substrates. However, the yellow edible ink was chosen as a solvent, due to the compatibility with the desktop printer, which ensured proper droplet ejection. The addition of vitamin Bs might have slightly increased the viscosity of the solution. Yet, this was not seen to affect the printing result based on visual perception comparing the yellow squares with and without vitamins.

Due to the variable results gained from the LC-MS method regarding the printed doses, the colorimetry results were mainly presented as a function of printed layers. The colorimetric method was seen to be sensitive to detect color differences ( $\Delta E^*_{ab}$ ) of layer addition up to the 5th printed layer for SP and 6th printed layer for CP and RP, with the ink formulation setup used. Because of the high color intensity difference between the pure substrate and the first layer, the pure substrate could not be used as a reference for the colorimetry measurements. Optimization of the color addition, to obtain a less color-intense ink, would enable the use of the pure substrate as a reference. Furthermore, evaluation of the operational window of the color escalation would need to be done in the future to avoid reaching the color saturation point within the planned dose interval. Previously, a water-based riboflavin (B<sub>2</sub>) ink, with glycerol as viscosity modifier, was printed using two different office printers (41). The printed samples of six different intensities were visually analyzed using an Olympus B2 microscope. A sensation of color intensity differences was observed for the low-intensity samples, while color saturation occurred, as also in the present study, for the samples with high color intensities.

The substrate properties were seen to have a major impact on the measured L\* values contributing to the calculated  $\Delta E^*_{ab}$  values gained from the colorimeter. This could for instance be seen for the higher  $\Delta E^*_{ab}$  values measured for RP, compared to the lower values measured for CP and SP. The lightness originated from the white and opaque substrates and was seen to decrease as more layers of the yellow vitamin B ink were applied. The rather large change of 8  $\mu\text{m}$  (pure RP vs. five layers of ink) for Sq-R and almost 3  $\mu\text{m}$  for Sq-W could explain the higher  $\Delta E^*_{ab}$  values for the specific formulation. When comparing the two edible substrates, the best dose escalation was reported for the porous RP, but the smallest standard deviations with regard

to the  $\Delta E^*_{ab}$  values and the colorimetry method were noted for SP.

### Quality Control Using Handheld Devices

The use of different handheld IR, NIR, and Raman spectroscopic devices for rapid and non-destructive quality control has recently been studied (25, 42, 43). Differentiation between pharmaceutical products of different strengths was shown to be possible using a handheld Raman device (43). A handheld counterfeit detector device (CD-3) with LEDs of various wavelengths and a laser-emitting photometric device, named counterfeit drug indicator (CoDI), were shown to be able to detect counterfeit antimalarial tablets (25). Furthermore, the CD-3 device was seen to provide information about how the samples had been stored based on the measured differences in fluorescence. In the same study, a colorimetric method was used as a control to identify and quantify the API in a laboratory environment. In this study, the usability of the handheld colorimeter Eoptis was evaluated for identification of doses with different color intensities. Values corresponding to the CIELAB color space were only gained from the handheld device, and thus, quantification of the APIs based on absorbance intensities was not possible. The method was seen to be applicable in differentiating flexible doses until color saturation occurred. Since the colorimetric method as such is not specific for a drug or a drug combination, validation needs to be done for each formulation to be measured and controlled by the handheld device. The concept of being able to perform quality control measurements with a handheld device supports well the advances in printing of personalized doses at the PoC (44). Handheld IR, NIR, and Raman spectroscopic devices could for instance be used to perform both quantitative and qualitative measurements at different stages in the distribution chain. The use of a colorimeter would be fast and cost-effective, enabling the healthcare professionals distributing the medicine (e.g., a nurse or a pharmacist) to differentiate between different doses of colored pharmaceuticals and to check prior to administration that the right dose required for individual pediatric patients was printed on the edible substrate.

### CONCLUSION

Colorimetry was shown to be an applicable method to identify flexible doses with regard to their different color intensities. Yet, optimization of the formulation has to be done in order to avoid reaching color saturation within the planned dose interval. The use of a handheld colorimeter would be a convenient low-cost and fast method for differentiation of printed age-appropriate and personalized doses for pediatrics prepared at the PoC. SWLI was seen to be a viable non-contact and non-destructive method to be utilized in the research and development of printed pharmaceuticals to understand the surface properties of the substrates as well as the effect of pharmaceutical ink deposition on the roughness of the substrates.

### ACKNOWLEDGEMENTS

The funding from Tor, Joe och Pentti Borg Fond is greatly acknowledged. Emrah Yildir is thanked for showing



the Lorentzen & Wettre micrometer device used for substrate thickness measurements.

## REFERENCES

- World Health Organization. Guidelines on submission of documentation for a multisource (generic) finished pharmaceutical product for the WHO Prequalification of Medicines Program: quality part. WHO Expert Committee on Specifications for Pharmaceutical Preparations. 46th report. Geneva. 2012; Annex 5:200–204. [http://www.who.int/medicines/areas/quality\\_safety/quality\\_assurance/expert\\_committee/TRS-970-pdf1.pdf](http://www.who.int/medicines/areas/quality_safety/quality_assurance/expert_committee/TRS-970-pdf1.pdf) Accessed 12 Aug 2016.
- Ernest TB, Craig J, Nunn A, Salunke S, Tuleu C, Breikreutz J, *et al.* Preparation of medicines for children—a hierarchy of classification. *Int J Pharm.* 2012;435(2):124–30. doi:10.1016/j.ijpharm.2012.05.070.
- Nahata MC, Allen LV. Extemporaneous drug formulations. *Clin Ther.* 2008;30(11):2112–9. doi:10.1016/j.clinthera.2008.11.020.
- Preis M, Pein M, Breikreutz J. Development of a taste-masked orodispersible film containing dimenhydrinate. *Pharmaceutics.* 2012;4(4):551–62. doi:10.3390/pharmaceutics4040551.
- Stoltenberg I, Breikreutz J. Orally disintegrating mini-tablets (ODMTs)—a novel solid oral dosage form for paediatric use. *Eur J Pharm Biopharm.* 2011;78(3):462–9. doi:10.1016/j.ejpb.2011.02.005.
- Klingmann V, Spomer N, Lerch C, Stoltenberg I, Frömke C, Bosse HM, *et al.* Favorable acceptance of mini-tablets compared with syrup: a randomized controlled trial in infants and preschool children. *J Pediatr.* 2013;163(6):1728–32. doi:10.1016/j.jpeds.2013.07.014.
- Buanz AB, Belaunde CC, Soutari N, Tuleu C, Gul MO, Gaisford S. Ink-jet printing versus solvent casting to prepare oral films: effect on mechanical properties and physical stability. *Int J Pharm.* 2015;494(2):611–8. doi:10.1016/j.ijpharm.2014.12.032.
- Voura C, Gruber MM, Schroedl N, Strohmeier D, Eitzinger B, Bauer W, *et al.* Printable medicines: a microdosing device for producing personalised medicines. *Pharm Technol Eur.* 2011;23(1):32–6.
- Preis M, Breikreutz J, Sandler N. Perspective: concepts of printing technologies for oral film formulations. *Int J Pharm.* 2015;494(2):578–84. doi:10.1016/j.ijpharm.2015.02.032.
- Genina N, Janßen EM, Breitenbach A, Breikreutz J, Sandler N. Evaluation of different substrates for inkjet printing of rasagiline mesylate. *Eur J Pharm Biopharm.* 2013;85(3):1075–83. doi:10.1016/j.ejpb.2013.03.017.
- Rajjada D, Genina N, Fors D, Wisaeus E, Peltonen J, Rantanen J, *et al.* A step toward development of printable dosage forms for poorly soluble drugs. *J Pharm Sci.* 2013;102(10):3694–704. doi:10.1002/jps.23678.
- Wickström H, Palo M, Rijckaert K, Kolakovic R, Nyman JO, Määttänen A, *et al.* Improvement of dissolution rate of indomethacin by inkjet printing. *Eur J Pharm Biopharm.* 2015;75:91–100. doi:10.1016/j.ejps.2015.03.009.
- Genina N, Fors D, Vakili H, Ihalainen P, Pohjala L, Ehlers H, *et al.* Tailoring controlled-release oral dosage forms by combining inkjet and flexographic printing techniques. *Eur J Pharm Sci.* 2012;47(3):615–23. doi:10.1016/j.ejps.2012.07.020.
- National Institutes of Health (NIH). Nutrient recommendations: dietary reference intakes (DRI) <https://ods.od.nih.gov/factsheets/list-VitaminsMinerals/> Accessed 12 Aug 2016.
- Kolakovic R, Viitala T, Ihalainen P, Genina N, Peltonen J, Sandler N. Printing technologies in fabrication of drug delivery systems. *Expert Opin Drug Deliv.* 2013;10(12):1711–23. doi:10.1517/17425247.2013.859134.
- Alomari M, Mohamed FH, Basit AW, Gaisford S. Personalised dosing: printing a dose of one's own medicine. *Int J Pharm.* 2015;494(2):568–77. doi:10.1016/j.ijpharm.2014.12.006.
- Vakili H, Kolakovic R, Genina N, Marmion M, Salo H, Ihalainen P, *et al.* Hyperspectral imaging in quality control of inkjet printed personalised dosage forms. *Int J Pharm.* 2015;483(1):244–9. doi:10.1016/j.ijpharm.2014.12.034.
- Hammes F, Hille T, Kissel T. Reflectance infrared spectroscopy for in-line monitoring of nicotine during a coating process for an oral thin film. *J Pharm Biomed Anal.* 2014;89:176–82. doi:10.1016/j.jpba.2013.10.047.
- Ayaz EA, Altintas SH, Turgut S. Effects of cigarette smoke and denture cleaners on the surface roughness and color stability of different denture teeth. *J Prosthet Dent.* 2014;112(2):241–8. doi:10.1016/j.prosdent.2014.01.027.
- Rossel RV, Minasny B, Roudier P, McBratney AB. Colour space models for soil science. *Geoderma.* 2006;133(3):320–37. doi:10.1016/j.geoderma.2005.07.017.
- Trinderup CH, Dahl A, Jensen K, Carstensen JM, Conradsen K. Comparison of a multispectral vision system and a colorimeter for the assessment of meat color. *Meat Sci.* 2015;102:1–7. doi:10.1016/j.meatsci.2014.11.012.
- Yagiz Y, Balaban MO, Kristinsson HG, Welt BA, Marshall MR. Comparison of Minolta colorimeter and machine vision system in measuring colour of irradiated Atlantic salmon. *J Sci Food Agric.* 2009;89(4):728–30. doi:10.1002/jsfa.3467.
- Wu D, Sun DW. Colour measurements by computer vision for food quality control—a review. *Trends Food Sci Technol.* 2013;29(1):5–20. doi:10.1016/j.tifs.2012.08.004.
- Facundo HV, Gurak PD, Mercadante AZ, Lajolo FM, Cordenunsi BR. Storage at low temperature differentially affects the colour and carotenoid composition of two cultivars of banana. *Food Chem.* 2015;170:102–9. doi:10.1016/j.foodchem.2014.08.069.
- Green MD, Hostetler DM, Nettey H, Swamidoss I, Ranieri N, Newton PN. Integration of novel low-cost colorimetric, laser photometric, and visual fluorescent techniques for rapid identification of falsified medicines in resource-poor areas: application to artemether–lumefantrine. *Am J Trop Med Hyg.* 2015;92(6 Suppl):8–16. doi:10.4269/ajtmh.14-0832.
- Steele G. Preformulation as an aid to product design in early drug development. In: Gibson M, editor. *Pharmaceutical preformulation and formulation.* 2nd ed. New York: Informa Healthcare USA, Inc; 2009. p. 206–7.
- Bhugra D, Ventriglio A, Till A, Malhi G. Colour, culture and placebo response. *Int J Soc Psychiatry.* 2015;61(6):615–7. doi:10.1177/0020764015591492.
- Leon K, Mery D, Pedreschi F, Leon J. Color measurement in L\* a\* b\* units from RGB digital images. *Food Res Int.* 2006;39(10):1084–91. doi:10.1016/j.foodres.2006.03.006.
- Tung FF, Goldstein GR, Jang S, Hittelman E. The repeatability of an intraoral dental colorimeter. *J Prosthet Dent.* 2002;88(6):585–90. doi:10.1067/mpr.2002.129803.
- CLM-194 User Guide, Digital handheld colorimeter, Eoptis, Rev. 1.04-03/2014.
- Yam KL, Papadakis SE. A simple digital imaging method for measuring and analyzing color of food surfaces. *J Food Eng.* 2004;61(1):137–42. doi:10.1016/S0260-8774(03)00195-X.
- Sandler N, Määttänen A, Ihalainen P, Kronberg L, Meierjohann A, Viitala T, *et al.* Inkjet printing of drug substances and use of porous substrates—towards individualized dosing. *J Pharm Sci.* 2011;100(8):3386–95. doi:10.1002/jps.22526.
- Genina N, Fors D, Palo M, Peltonen J, Sandler N. Behavior of printable formulations of loperamide and caffeine on different substrates—effect of print density in inkjet printing. *Int J Pharm.* 2013;453(2):488–97. doi:10.1016/j.ijpharm.2013.06.003.
- Buanz AB, Saunders MH, Basit AW, Gaisford S. Preparation of personalized-dose salbutamol sulphate oral films with thermal ink-jet printing. *Pharm Res.* 2011;28(10):2386–92. doi:10.1007/s11095-011-0450-5.
- Sheraz MA, Kazi SH, Ahmed S, Anwar Z, Ahmad I. Photo, thermal and chemical degradation of riboflavin. *Aubé J, ed. Beilstein J Org Chem.* 2014;10:1999–2012. doi:10.3762/bjoc.10.208.
- Hudd A. Inkjet printing technologies. In: Magdassi S, editor. *Chemistry of inkjet inks.* Singapore: WSPC; 2009. p. 7.
- Meléndez PA, Kane KM, Ashvar CS, Albrecht M, Smith PA. Thermal inkjet application in the preparation of oral dosage forms: dispensing of prednisolone solutions and polymorphic characterization by solid-state spectroscopic techniques. *J Pharm Sci.* 2008;97(7):2619–36. doi:10.1002/jps.21189.
- Sue-Chu M, Kristensen S, Tønnesen HH. Influence of lag-time between light exposure and color evaluation of riboflavin in the solid state. *Pharmazie.* 2008;63(7):545–6. doi:10.1691/ph.2008.8070.

39. Stark G, Fawcett JP, Tucker IG, Weatherall IL. Instrumental evaluation of color of solid dosage forms during stability testing. *Int J Pharm*. 1996;143(1):93–100. doi:10.1016/S0378-5173(96)04691-1.
40. Allam KV, Kumar GP. Colorants—the cosmetics for the pharmaceutical dosage forms. *Int J Pharm Pharm Sci*. 2011;3(3):13–21.
41. Takala M, Helkiö H, Sundholm J, Genina N, Kiviluoma P, Widmaier T, Sandler N, Kuosmanen P. Ink-jet printing of pharmaceuticals. In: Proceedings of the 8th International DAAAM Baltic Conference 2012 Apr 19.
42. Sorak D, Herberholz L, Iwascek S, Altinpinar S, Pfeifer F, Siesler HW. New developments and applications of handheld Raman, mid-infrared, and near-infrared spectrometers. *Appl Spectrosc Rev*. 2012;47(2):83–115. doi:10.1080/05704928.2011.625748.
43. Hajjou M, Qin Y, Bradby S, Bempong D, Lukulay P. Assessment of the performance of a handheld Raman device for potential use as a screening tool in evaluating medicines quality. *J Pharm Biomed Anal*. 2013;74:47–55. doi:10.1016/j.jpba.2012.09.016.
44. Preis M and Sandler N. Printing technologies and tailored dosing. *Hosp Healthc*. 2016;in press.